

# **Supporting Information:**

## **Multilamellar Vesicle Formation**

### **Probed by Rheo-NMR and Rheo-SALS Under Large Amplitude Oscillatory Shear**

Stefan Kuczera,<sup>†,‡</sup> Luigi Gentile,<sup>¶,‡</sup> Timothy I. Brox,<sup>†</sup> Ulf Olsson,<sup>‡</sup> Claudia Schmidt,<sup>§</sup> and Petrik Galvosas<sup>\*,†</sup>

*Victoria University of Wellington, SCPS, MacDiarmid Institute for Advanced Materials and Nanotechnology, Wellington, New Zealand, Division of Physical Chemistry, Lund University, P.O. Box 124, SE-221 00 Lund, Sweden, Department of Biology, MEMEG unit, Lund University, Sölvegatan 35, 223 62 Lund, Sweden, and Department of Chemistry, Paderborn University, Warburger Str. 100, D-33098 Paderborn, Germany*

E-mail: petrik.galvosas@vuw.ac.nz

There are 9 pages, 10 figures and 0 tables in this document.

---

\*To whom correspondence should be addressed

<sup>†</sup>Victoria University of Wellington

<sup>‡</sup>Division of Physical Chemistry, Lund University, P.O. Box 124, SE-221 00 Lund, Sweden

<sup>¶</sup>Department of Biology, MEMEG unit, Lund University, Sölvegatan 35, 223 62 Lund, Sweden

<sup>§</sup>Department of Chemistry, Paderborn University, Warburger Str. 100, D-33098 Paderborn, Germany

## Line shape model

The line shape model proposed by Medronho et al.<sup>1</sup> for the MLV peak is given by a sum of Lorentzian functions:

$$L(f) = \sum_{n=1}^N k_n \frac{2T_{2,n}}{1 + 4\pi^2(f - f_0)^2 T_{2,n}^2} . \quad (1)$$

$T_{2,n}$  is the transverse relaxation time associated with layer number  $n$  and  $f_0$  is the resonance frequency. The weights  $k_n$  are proportional to the volume of each layer and given by  $k_n = n^2 d^2$  where  $d$  is the ( $n$ -independent) layer spacing.  $T_{2,n}$  is expressed as

$$\frac{1}{T_{2,n}} = \frac{2\Delta f_Q^2 d^2}{15D} n^2 + \frac{1}{T_{2,\text{inhom}}} \quad (2)$$

within the model, where  $\Delta f_Q$  is the quadrupolar splitting of the lamellar phase and  $D$  the water self-diffusion coefficient. The additional term,  $1/T_{2,\text{inhom}} = \pi \Delta f_{1/2,\text{inhom}}$ , takes into account the effect of the magnetic field inhomogeneity on the line shape defined by a line width at half height  $f_{1/2,\text{inhom}}$ .  $f_{1/2,\text{inhom}}$  was estimated from the sponge phase spectrum to be 50 Hz .

In order to fit the model to the spectra obtained in the experiments the fit function

$$f_{\text{fit}}(f; N, c) = c \cdot \frac{1}{Nd^2} \cdot L(f, N) \quad (3)$$

was used with  $c$  being a scaling factor. The values for  $d = 6.5 \mu\text{m}$  and  $D = 10^{-9} \text{m}^2/\text{s}$  were chosen as in Medronho et al.<sup>1</sup>, whereas  $\Delta f_Q$  was taken from the corresponding lamellar spectra recorded directly before the start of shear. This leaves  $N$  and  $c$  as the optimization parameters. In contrast to Medronho et al.<sup>1</sup>, where agreement was judged by the eye, a simplex optimizer algorithm has been applied to fit  $f_{\text{fit}}$ . The scaling  $1/N$  of the spectra was necessary to make the fitting algorithm work, which can not handle integer values (as  $N$  is for the sum). From the fitted values the MLV radius can be calculated as  $R_{\text{MLV}} = Nd$ .

## Lorentzian fits

Model function used for single Lorentzian fit:

$$L(f) = I_1 \frac{w_1/2}{(w_1/2)^2 + (f - c_1)^2} \quad (4)$$

$I_1$  is the area (intensity) of the MLV peak,  $w_1$  is the width of the MLV peak and  $c_1$  is the peak centre.

Double Lorentzian:

$$L(f) = I_2 \left( \frac{w_2/2}{(w_2/2)^2 + (f - c_2)^2} + \frac{w_2/2}{(w_2/2)^2 + (f - c_3)^2} \right) \quad (5)$$

$I_2$  is the (shared) area (intensity) of the (lamellar) double peak,  $w_2$  the (shared) width of the lamellar peaks and  $c_{2,3}$  are the respective peak centres.

## NMR imaging

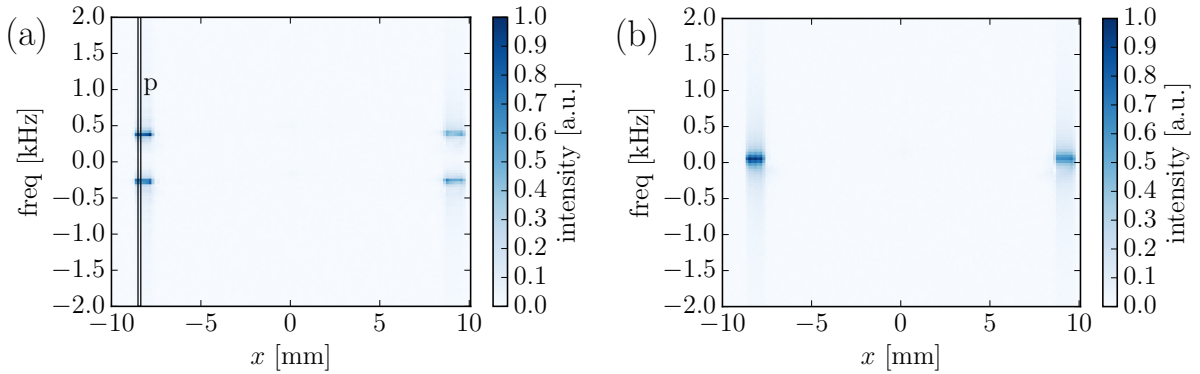


Figure S1: Sample 1D spectra maps acquired with the sequence shown in Fig. 1c of the article in lamellar (a) and MLV (b) state. In (a) the pixel used for comparison of NMR spectra is indicated by the rectangle marked with ‘p’. The intensity differences between the left and right hand gap might be due to field inhomogeneities in the rf coil.

## Absolute strain

In theory the imposed strain  $\gamma_i(t)$  and shear rate  $\dot{\gamma}_i(t)$  can be described by the following expressions:

$$\gamma_i(t) = \gamma_0 \sin(\omega t + \varphi) + c , \quad (6)$$

and

$$\dot{\gamma}_i(t) = \gamma_0 \omega \cos(\omega t + \varphi) . \quad (7)$$

where  $\gamma_0$  is the strain amplitude and  $\omega$  the (angular) frequency. The phase  $\varphi$  and the strain offset  $c$  depend on the condition at  $t = 0$ . In our experiments we usually start with zero velocity without any preshear. Therefore

$$\gamma_i(0) = \dot{\gamma}_i(0) = 0 . \quad (8)$$

Consequently  $\varphi = -\pi/2$  (or  $\pi/2$ ) and  $c = \gamma_0$  (or  $-\gamma_0$ ).

To allow for comparison with steady shear experiments, the absolute shear  $\gamma(t)$  shall be defined as

$$\gamma(t) = \int_0^t |\dot{\gamma}_i(t')| dt' ; \quad (9)$$

see Fig. S2 for a graphical description. It is further assumed that the sample is not undergoing any structural transformation during the rest period. Thus the start-stop procedure is assumed to be equivalent to that of continuous oscillatory shear (as employed by the rheo-SALS experiments) with respect to the phase transformation.

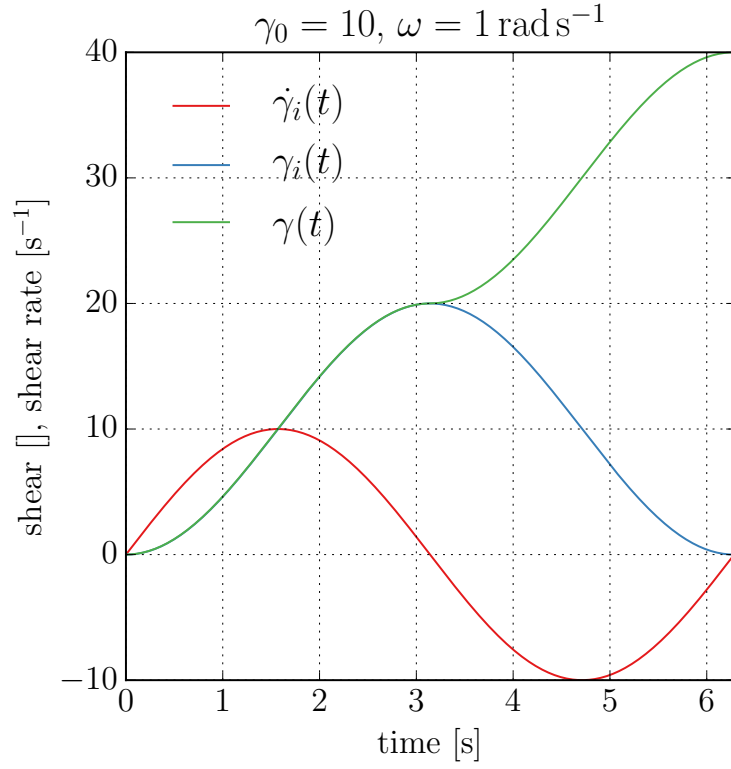


Figure S2: Theoretical curves for  $\gamma_i$ ,  $\dot{\gamma}_i$  and the absolute shear  $\gamma$  at  $\gamma_0 = 10$  and  $\omega = 1 \text{ rad s}^{-1}$  for one oscillation period. The absolute shear for one period is always  $4\gamma_0$ .

## MLV evolution process, NMR data

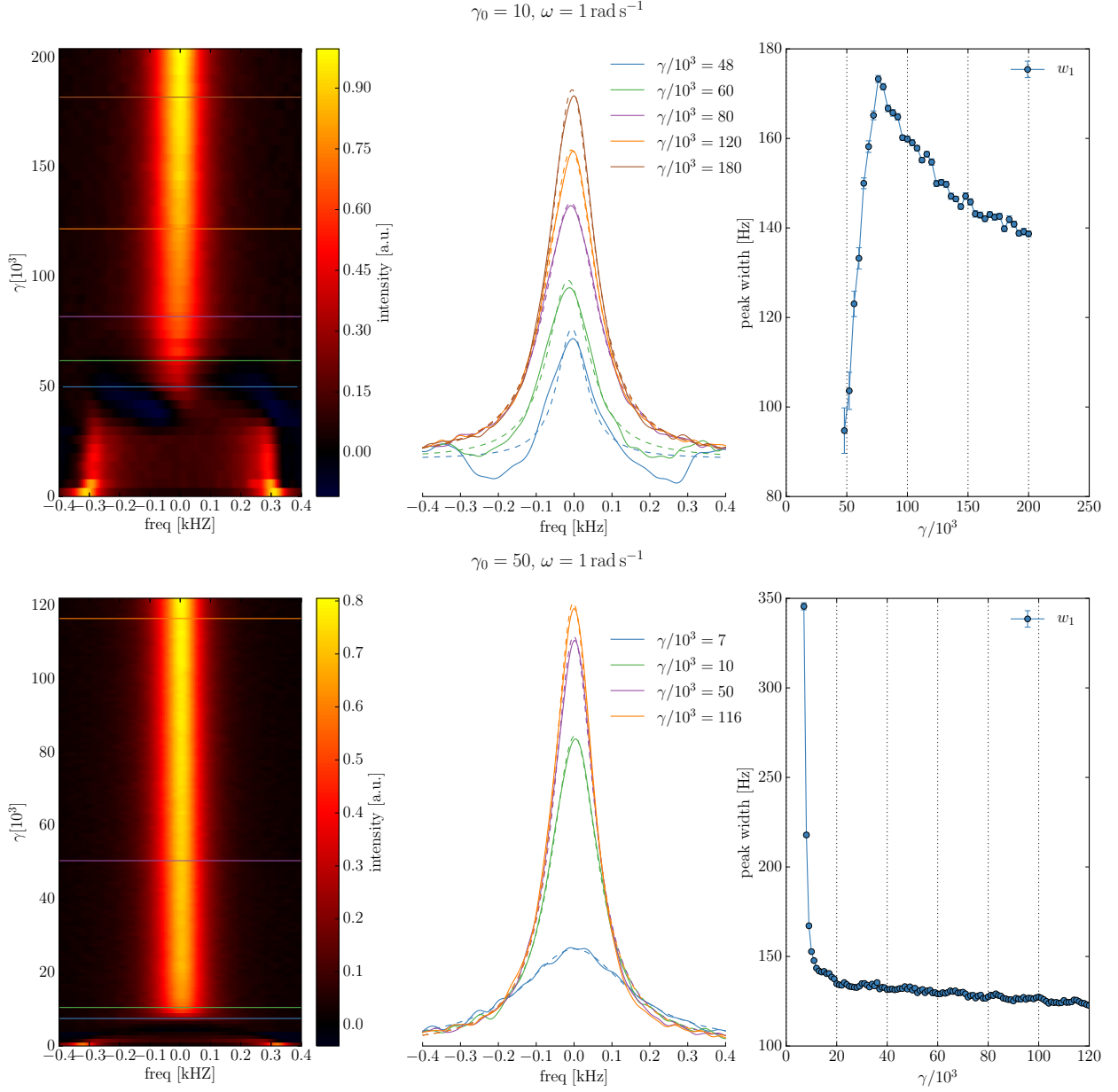


Figure S3: Left: Evolution of the NMR spectra for  $\omega = 1 \text{ rad s}^{-1}$  and  $\gamma_0 = 10$  (top) and  $\gamma_0 = 50$  (bottom). Center: Selected NMR spectra for  $\gamma$  values as indicated by horizontal lines on the left hand side. Dashed lines are Lorentzian fits. Right: Widths of the Lorentzian fits as a function of the absolute strain.

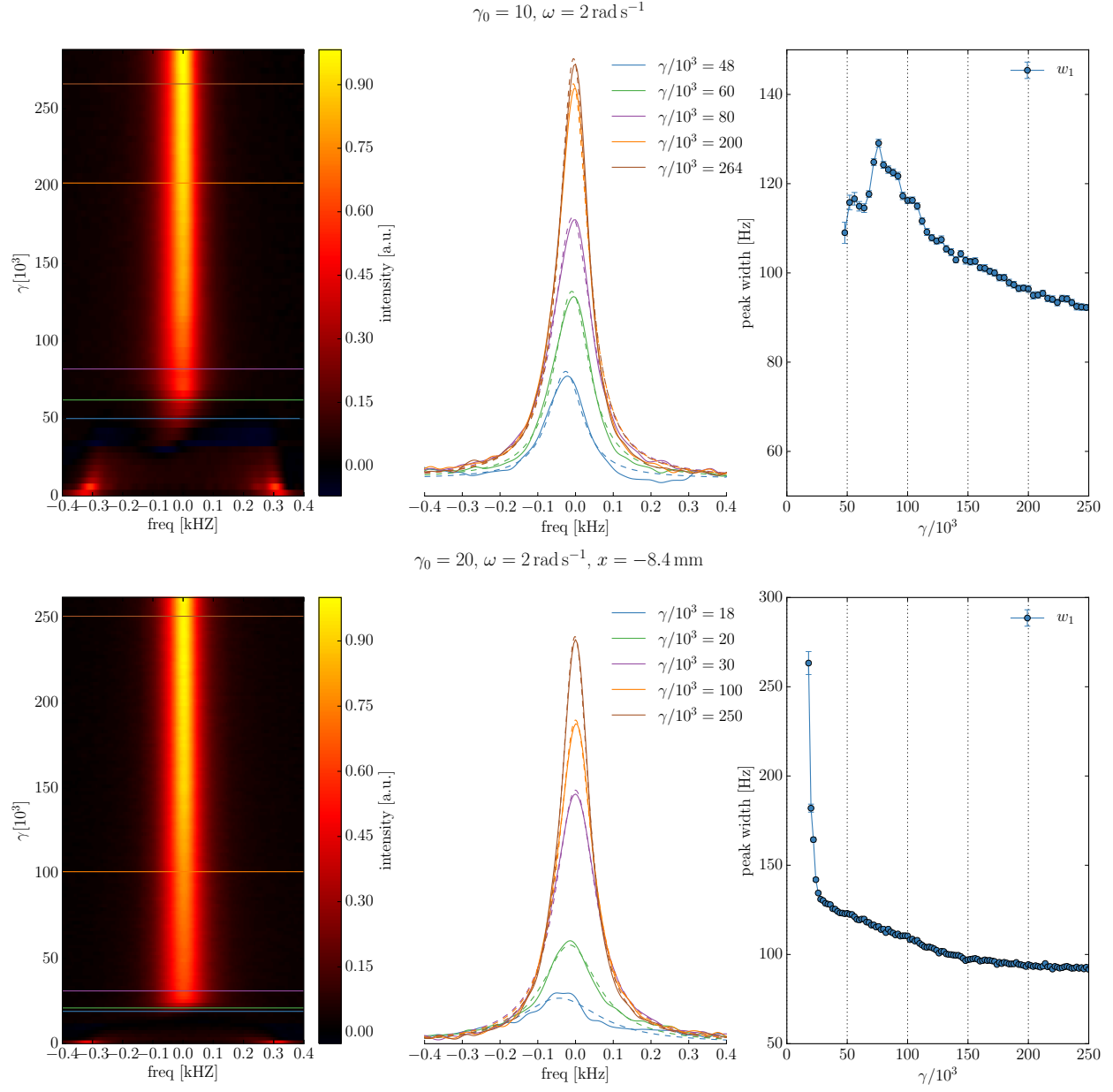


Figure S4: Left: Evolution of the NMR spectra for  $\omega = 2 \text{ rad s}^{-1}$  and  $\gamma_0 = 10$  (top) and  $\gamma_0 = 20$  (bottom). Center: Selected NMR spectra for  $\gamma$  values as indicated by horizontal lines on the left hand side. Dashed lines are Lorentzian fits. Right: Widths of the Lorentzian fits as a function of the absolute strain.

## MLV evolution process, SALS data

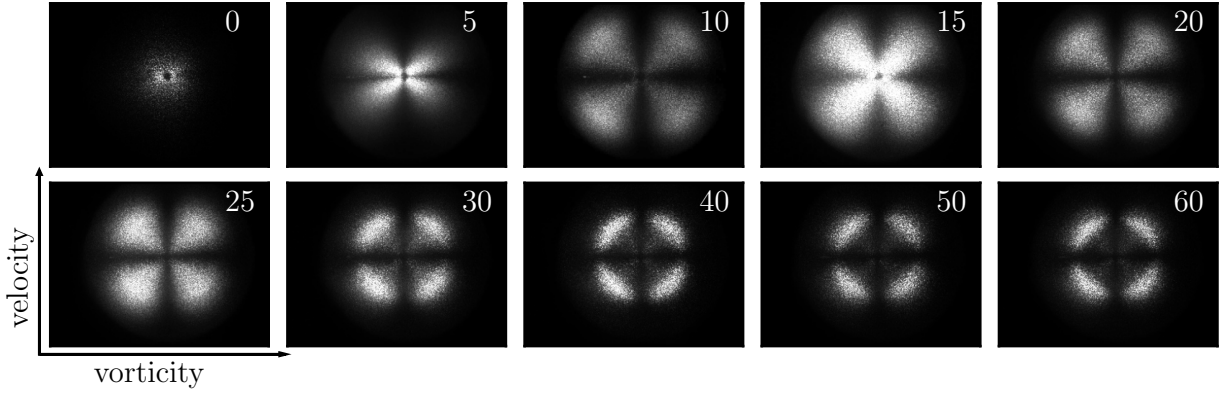


Figure S5: Evolution of the SALS pattern for  $\omega = 1 \text{ rad s}^{-1}$  and  $\gamma_0 = 30$  with absolute strain ( $\gamma/10^3$  indicated in each plot). All patterns were recorded at the same oscillatory phase with maximum shear rate ( $\dot{\gamma}(\gamma) = \dot{\gamma}_{\text{max}}$ ).

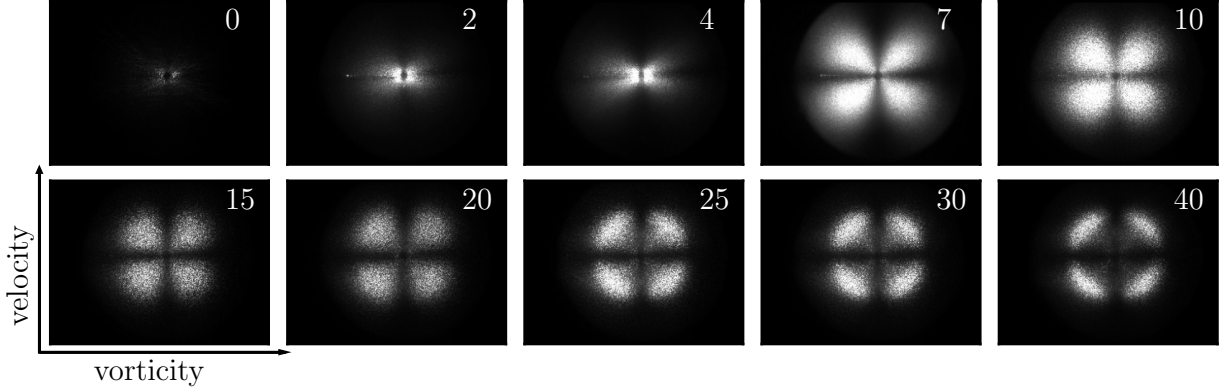


Figure S6: Evolution of the SALS pattern for  $\omega = 1 \text{ rad s}^{-1}$  and  $\gamma_0 = 50$  with absolute strain ( $\gamma/10^3$  indicated in each plot). All patterns were recorded at the same oscillatory phase with maximum shear rate ( $\dot{\gamma}(\gamma) = \dot{\gamma}_{\text{max}}$ ).



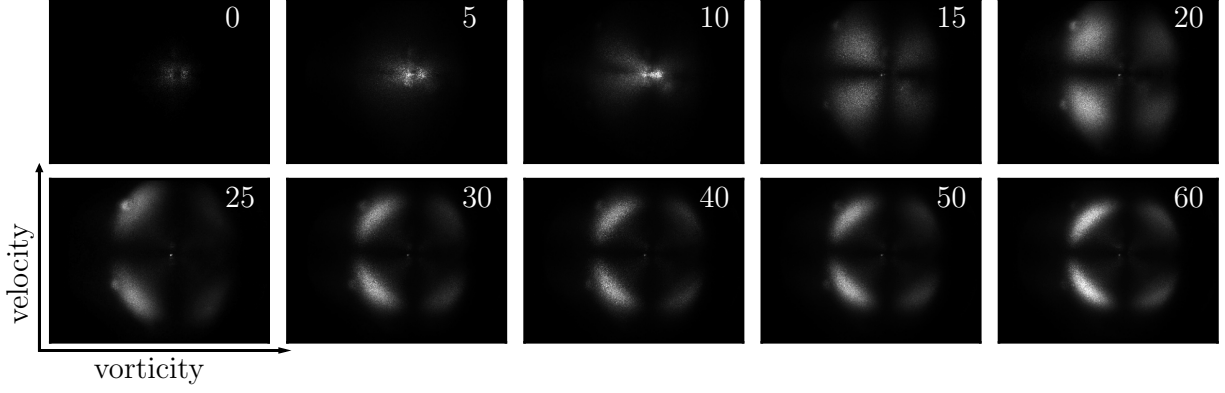


Figure S7: Evolution of the SALS pattern for  $\omega = 2 \text{ rad s}^{-1}$  and  $\gamma_0 = 20$  with absolute strain ( $\gamma/10^3$  indicated in each plot). All patterns were recorded at the same oscillatory phase with maximum shear rate ( $\dot{\gamma}(\gamma) = \dot{\gamma}_{\text{max}}$ ).

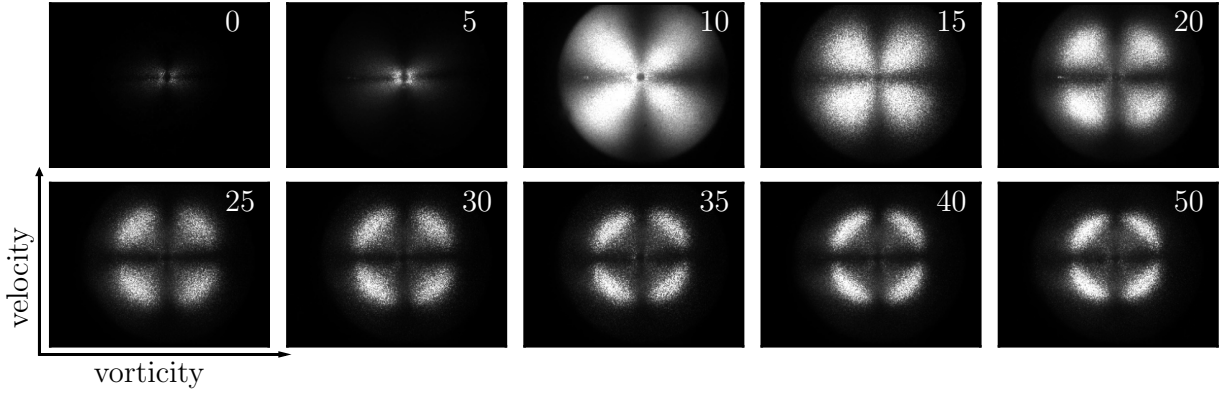


Figure S8: Evolution of the SALS pattern for  $\omega = 2 \text{ rad s}^{-1}$  and  $\gamma_0 = 30$  with absolute strain ( $\gamma/10^3$  indicated in each plot). All patterns were recorded at the same oscillatory phase with maximum shear rate ( $\dot{\gamma}(\gamma) = \dot{\gamma}_{\text{max}}$ ).

## SALS of intermediate state under steady shear

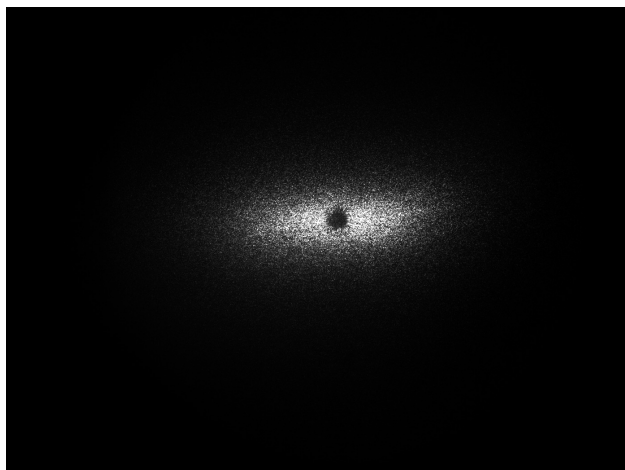


Figure S9: SALS pattern of the intermediate state resembling multilamellar cylinders observed during the application of steady shear ( $10\text{ s}^{-1}$ ).

## Lissajous pattern under SAOS

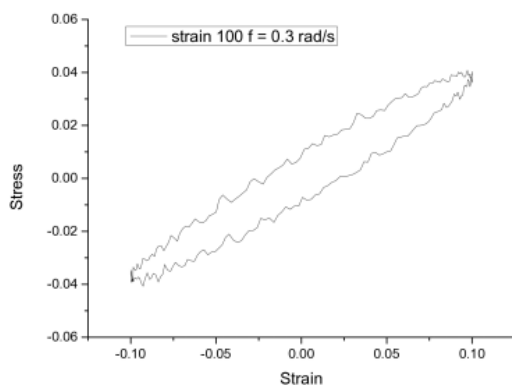


Figure S10: Lissajous curve for a SAOS experiment on a pure state of aligned lamellae. The sample was presheared up to a total strain of 100 to achieve alignment of the layers.

## References

- (1) Medronho, B.; Schmidt, C.; Olsson, U.; Miguel, M. G. Size Determination of Shear-Induced Multilamellar Vesicles by Rheo-NMR Spectroscopy. *Langmuir* **2010**, *26*, 1477–1481.